Current Issues in Organic Chemistry
eds. K. Hadjiivanov, V. Valtchev, S. Mintova, G. Vayssilov
Heron Press, Sofia, 2010

A Comparison of the Stucture Characteristics of the Hydrogels Used for the Synthesis of LTA and MFI Zeolites

C. Kosanović[1], **K. Havancsák**[2], **B. Subotić**[1], **V. Svetličić**[1], **T. Mišić**[2], **Á. Cziráki**[2], **G. Huhn**[2]

[1]Ruđer Bošković Institute, 10000 Zagreb, Croatia

[2]Dept. of Materials Physics, Eötvös Univ., H-1117 Budapest, Hungary

Abstract

Solid phase (gel) separated from freshly prepared hydrogel having the batch molar composition: 2.5Na_2O-8TPABr-60SiO_2-800H_2O as well as the solids drawn off the reaction mixture, during its hydrothermal treatment at 443 K and solid phase (gel) separated from freshly prepared hydrogel having the batch molar composition: $0.468Na_2O \times Al_2O_3 \times 3.382SiO_2 \times 55.44H_2O$ as well as the solids drawn off the reaction mixture, during its hydrothermal treatment at 353 K were analyzed by different methods such as powder X-ray diffraction (XRD), Fourier transform infrared spectroscopy (FTIR), scanning-electron microscopy (SEM), transmission electron microscopy (TEM), electron diffraction (ED) and atomic force microscopy (AFM). It has been found that the first mentioned freshly prepared gel represents a "hierarchical structure" in which the largest individual gel aggregates (having the size 200–1000 nm, or more) are composed of smaller particles having the size in the range 40–80 nm, which represent aggregates of $\leqslant 10$ nm particles. The second gel is mainly composed of disc-shaped primary particles as well of partially or even fully crystalline entities. The nuclei formed inside both the gel particles and/or small nanocrystals formed by a limited grow of nuclei in the gel matrix, can grow only after their release from the gel dissolved during the crystallization, i.e. when they are in full contact with the liquid phase.

1 Introduction

Synthesis of zeolites is following a complex of mechanisms and processes due to the hydrothermal crystallization. The reactions occur in multicomponent systems where interactions, chemical reactions, equilibrium, crystal nucleation and growth processes are taking place. During the crystallization these processes are changed with time pass.

The type of zeolite to be crystallized, depends to a large extent on the chemical composition of its precursor and the mode of its preparation, and to a lesser

extent, on the crystallization conditions [1,2]. In both cases, crystallization takes place by formation of primary zeolite particles (nuclei) and their solution-mediated growth from solution supersaturated with active aluminate, silicate and aluminosilicate anions [1]. While the mechanism of the crystal growth of zeolites is well defined by the reactions of active aluminate, silicate and/or aluminosilicate species from the liquid phase on the surface of growing zeolite crystals [3] and revealed by numerous AFM studies [4-7], there is still much uncertainty regarding the relevant mechanisms of zeolite nucleation [1]. Although various nucleation mechanisms such as homogeneous [8], heterogeneous [9] and secondary nucleation [10] in the liquid phase supersaturated with soluble aluminate, silicate and aluminosilicate species as well as a nucleation process on the gel/liquid interface [11] have been proposed as the processes relevant for the formation of primary zeolite particles, there is abundant experimental evidence that due to the high supersaturation of constituents (Na, Si, Al, template) in gel [12,13], a considerable amount of nuclei are formed in the gel and/or at the gel/liquid interface by a linking of specific subunits during gel precipitation and/or ageing [14-17].

The formation of nuclei in the gel phase as was originally proposed by Flanigen and Breck [18] is followed by crystallization through depolymerization and rearrangement of the gel network, mediated by OH^- ions. The same assumption was mentioned by a lot of authors [19-24] although Flaningen came later with the theory that the nucleation of low silica zeolites undergo by solution chemistry, while high silica zeolites nucleate in the gel [25].

In the other hand Derouane and others showed that ZSM-5 is depending on the preparation conditions and the source of reactants could grow either from solution or gel [26].

De Moor and others [27] proved evidence of the nucleation mechanism of an organi-mediated synthesis of MFI zeolite (see Figure in Ref. [27]). They show that 2.8 nm entities, comprised of TPA and silicate act as primary building units that aggregate to form structure up to 10 nm in size, that form the nuclei for the crystallization of zeolite. Schoeman monitored the early stages of TPA-silicalite using dynamic light scattering (DLS). He also detected subcolloidal particles in the solution of about 2.5–3.3 nm which are assumed to be the starting entities having short range order [28].

In this study are investigated the microstructural particularities of the amorphous aluminosilicate and silicate precursors used for the synthesis of LTA and MFI zeolites using AFM as the main experimental method in combination with spectroscopic methods (FT-IR, XRD), microscopic methods (SEM, HR-TEM) and other techniques (DTG, DSC). The Si-source for preparing the silicate solution was for both the precursors fumed silica for better comparison.

2 Experimental

2.1 Samples preparation

Silicate precursor for the MFI zeolite synthesis

The gel with molar batch composition: 2.5Na_2O-8TPABr-60SiO_2-800H_2O was prepared by mixing of the reagents in the following order: freshly prepared 30% NaOH solution; TPABr; demineralised water; and fumed silica. Freshly prepared gel ($t_c = 0$) was centrifuged immediately after preparation. After removal of the supernatant, the solid phase was redispersed in demineralized water and centrifuged repeatedly. The procedure was repeated until the pH value of the liquid phase above the sediment was 9. The wet washed solids were dried overnight at 378 K and cooled in a desiccator over silicagel.

Aluminosilicate precursor for the LTA zeolite synthesis

The aluminosilicate hydrogel with molar batch composition: 0.468$Na_2O\times$ $Al_2O_3\times$3.382$SiO_2\times$55.44H_2O was prepared by mixing together the appropriate Na-silicate and Na-aluminate solutions at room temperature. Sodium silicate solution having appropriate concentrations of Na_2O and SiO_2 was prepared by dissolution of fumed silica in NaOH solution. Sodium aluminate solution having appropriate concentrations of Na_2O and Al_2O_3 was prepared by dissolution of aluminum wire in NaOH solution. Hydrogel was centrifuged to separate the solid amorphous phase from the liquid phase (supernatant). After removal of the supernatant, the solid phase was redispersed in demineralized water and centrifuged repeatedly. The procedure was repeated until the pH value of the liquid phase above the sediment was 9. The wet washed solids were dried overnight at 378 K and cooled in a desiccator over silicagel.

2.2 Sample analysis/characterization

The solid samples prepared as described above were characterized by the following techniques:

X-ray powder diffraction (XRD)

To obtain the X-ray diffraction patterns, the samples were analyzed in the angle range $2\theta = 5^\circ - 90^\circ$ with a scan rate of 0.001°/s, using X'Pert diffractometer (Philips).

Fourier Transform Infrared Spectroscopy (FTIR)

Infrared transmission spectra of the samples were made by the KBr wafer technique. The spectra were recorded on an FTIR. Spectrometer System 2000 FT-IR (Perkin-Elmer).

Scanning-Electron Microscopy (SEM)

The scanning-electron micrographs of the samples were taken by Philips XL 30 scanning-electron microscope.

Transmission Electron Microscopy (TEM)/Electron Diffraction (ED)

A powdered sample was mixed with ethanol and a drop of suspension was placed on a lacy carbon-coated Cu grid. Samples were examined by a Philips

CM 20 transmission electron microscope operated at 200 kV. TEM images and the selected area electron diffraction (SAED) method were used for determining the crystallinity of samples.

Atomic Force Microscopy (AFM)

The powdered sample was suspended in ultra-pure water (1 g/L) and stirred for one hour. The suspension was diluted in ultra-pure water so that the final suspension contained 10 mg of powder/L. Five μL of the final suspension were pipetted directly onto freshly cleaved mica. Following deposition, the mica sheets were placed in enclosed Petri dishes for several hours at a relative humidity of 50% in order to evaporate the excess of water. AFM imaging was performed using Multimode Scanning Probe Microscope with Nanoscope IIIa controller (Veeco Instruments, Santa Barbara, CA) with a vertical engagement (JV) 125 μm scanner. Images were collected using mainly tapping mode AFM because it is particularly well adapted to soft samples due to a nearly complete reduction of lateral forces. "Light tapping" was applied using silicon tips (TESP, Veeco) and silicon nitride (NP-20, Veeco) for contact mode. While imaging in contact mode the minimum force to maintain contact between the probe and the scanned surface was used.

Thermal Analysis

Thermogravimetric ($t.g.a.$) of gels was performed on a SDT 2960 thermal analysis system (TA Instruments, Inc.). The measurements were carried out in nitrogen flow with a heating rate of 10°C/min.

Chemical Composition

The composition of the gel was determined using EDS (contents of Na, Al, Si) and thermal analysis (H_2O content).

3 Results and Discussion

The solid phase separated from freshly prepared hydrogels used for the synthesis of silicalite-1 (MFI) and zeolite A (LTA) have been analyzed by different spectroscopic, microscopic and other methods. In the synthesis of silicalite, as structure directing agent, TPABr (tetrapropylammonium bromide) is used. The alkyl chains of TPA^+ cation and the hydrophobic silicate species join together through Van der Waals forces resulting in an inorganic-organic composite. Figure 1 shows that the nature of the samples (Aa,b) drawn of the reaction mixture at $t_c = 0$ is amorphous. Since IR vibrations of zeolite skeleton are intense for agglomerates of even few unit cells [29], the absorption peak at 571 cm^{-1} (Figure 1 Aa) implies the presence of ordered pentasile structure [29-31] in the precipitated gel precursor. According to Lesthaeghe *et al.* [32], this absorption peak corresponds to 36T of MFI structure. The absence of the intense band at 556 cm^{-1} that is assigned to external vibrations related to D-4 rings in zeolite A framework is indicating the amorphous nature of the gel but the weak broad band at about 589 cm^{-1} (Figure 1 Ab) could be assigned to the presence of nano-sized, partially crystalline ("quasi-crystalline") particles. The XRD pattern of the freshly precipitated gel precursor for the synthesis of silicalite-1

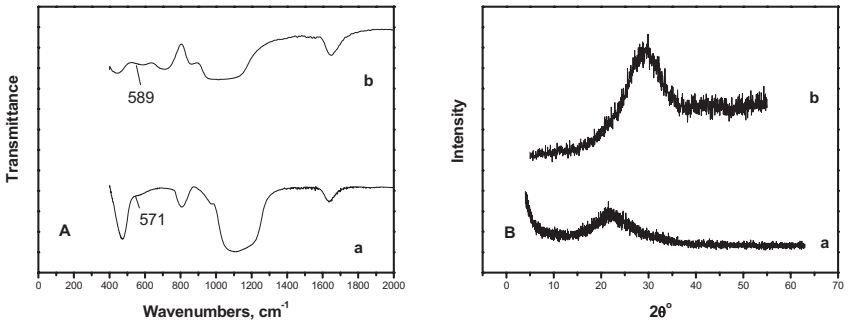

Figure 1. FTIR spectra (A) and X-ray diffraction patterns (B) of freshly precipitated amorphous precursors for the synthesis of silicalite-1 (a) and zeolite A (b).

(Figutr 1 Ba) shows a broad amorphous maximum around $2\Theta \sim 23^\circ$ and the XRD pattern of the freshly precipitated gel precursor for the synthesis of zeolite A1 (Figure 1 Bb) shows a broad amorphous maximum around $2\Theta \sim 29.5^\circ$ indicating that the materials are X-ray amorphous aggregates.

Figure 2 shows the SEM images of the X-ray amorphous precursors. The two gels precursors are consisted of multi-level aggregates which are obviously composed of smaller particles. TEM image, taken on the sample of the gel precursor for the synthesis of silicalite-1 (Figure 3 A), clearly indicates that the 40–80 nm gel particles are composed of smaller discrete spherical particles characterized by a diameter less than 10 nm. TEM image, taken on the sample of the gel precursor for the synthesis of zeolite A (Figure 3 Ba), shows that the sample is consists of unit globular features of 20–50 nm in size. The appearance of few faint diffraction circles in the electron diffraction pattern of the same gel (Figure 3 Bb) indicates that the X-ray amorphous solid contains particles of partially or "quasi-crystalline" phase having size below the X-ray diffraction limit but above the electron diffraction detection limit [33].

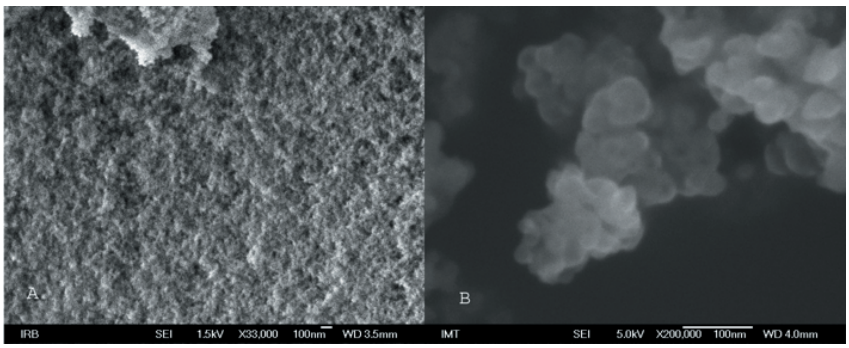

Figure 2. Scanning electron micrograph of the solid phase (gel) separated from the freshly prepared hydrogel for the synthesis of silicalite-1 (A) and for the synthesis of zeolite A (B).

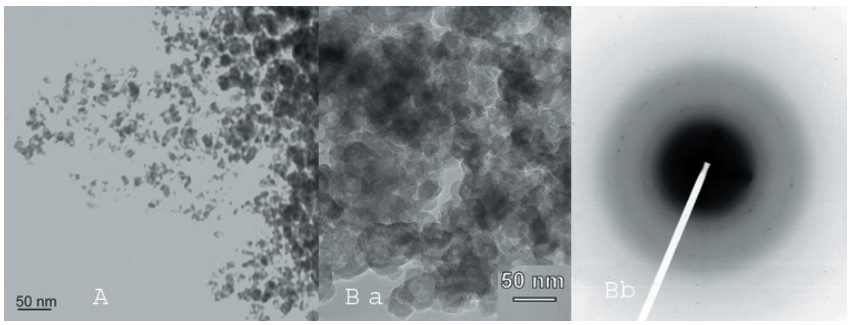

Figure 3. TEM image of the solid phase (gel) separated from the freshly prepared hydrogel for the synthesis of silicalite-1 (A) and for the synthesis of zeolite A (Ba). Electron-diffraction pattern of the solid phase separated from the reaction mixture for the synthesis of zeolite A (Bb), $t_c = 0$ h.

Since atomic force microscopy enables the detailed observation of nanometer-sized events, the gels are additionally analyzed by this method. The AFM section analysis of particles of the solid phase separated from the gel precursor for the synthesis of silicalite-1 (Figure 4) shows a specific profile with

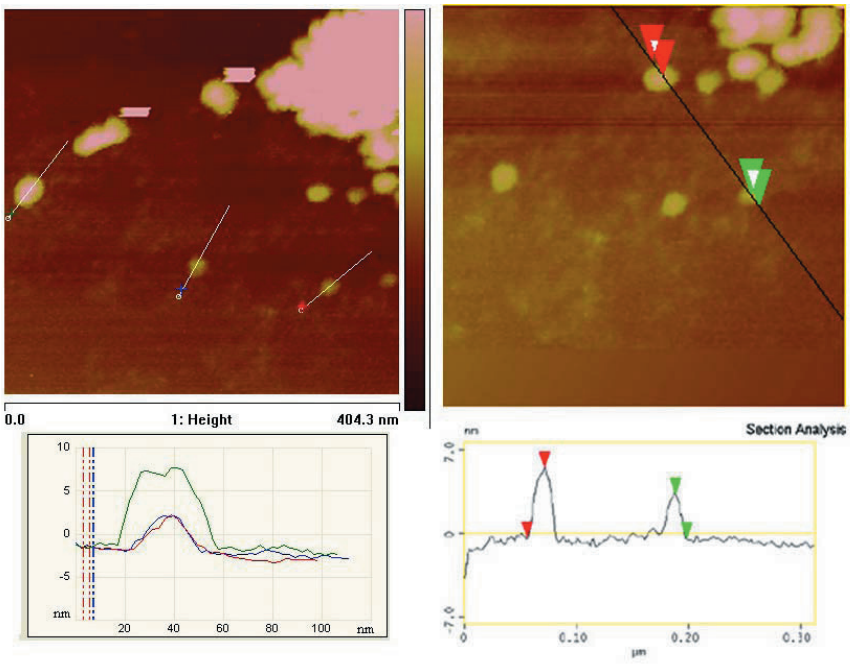

Figure 4. AFM image of the particles aggregates in the solid phase separated from a freshly prepared hydrogel used as precursor for the synthesis of silicalite-1 (gel; $t_c = 0$). Top view of height data and section analysis of the particles.

size of 40–50 nm. These measurements revealed that the diameter of the smallest particles is less than 10 nm. The particle diameter in the AFM measurements has been estimated following the procedure given in Ref. [34]. Although the height measurement is accurate, the apparent particle diameter is broadened by the finite dimensions of the probe tip. It is evident that the gel precursor represents a hierarchical structure, which has also been found in [35]. The largest (> 200 nm) individual gel aggregates (earlier also found in more "concentrated" heterogeneous systems [36]) consist of aggregates of smaller particles (40–80 nm), which also contain aggregates of particles $\leqslant 10$ nm. It is very certain that these particles $\leqslant 10$ nm are, in fact, the entities earlier identified as "6.4–7.2 nm fractal aggregates" [37], "globular structural units" [30] and the "(5–10) nm "secondary units" [36]. In this context, it is reasonable to assume that the gel particles $\leqslant 10$ nm in the hydrogels systems are formed in a similar or the same way as the secondary units [36] fractal aggregates [37], globular structural units [38] observed during crystallization of silicalite-1 from clear TPA-silicate solutions [39], namely by a stepwise aggregation of "primary (≈ 3 nm) units" composed of inorganic-organic composite species [36]. However, since the concentration of reactants in hydrogel is considerably higher than in clear solution, the aggregation of "primary (≈ 3 nm) units" into the secondary ones ($\leqslant 10$ nm) is very fast process, terminated during preparation of hydrogel, the $\leqslant 10$ nm particles are the smallest entities present in the system, as can be observed by TEM (Figure 3 A) and AFM (Figure 4).

Figures 5 and 6 show typical AFM image of the elemental (unit) particles of the solid phase separated from the gel precursor for the synthesis of zeolite A, on mica. The particles have diameter in the range from 50 nm to 120 nm (mainly 80 nm) and height from 8 nm to 20 nm (mainly 15 nm) which is considerably higher than the cross-section diameters measured by TEM (10–50 nm, see Figure 3). AFM image in Figure 5 contains three different types of nano-sized entities: a) near-spheroidal shaped particles, b) particles of quasi-crystalline phase and c) pyramidal-shape features that are believed to be the nuclei of zeolite which start to grow after their release from the gel matrix, when they are in full contact with the liquid phase. The difference in the particle size measured by the two methods (TEM, AFM) was probably caused by different ways of sample preparation and measuring conditions; while TEM requires dehydrated samples and imaging under vacuum, the sample for AFM was suspended in water prior to the deposition on mica and imaging was kept under ambient conditions (50% humidity and normal pressure; see Experimental). This implies that original size of the moist "primary" particles (50–120 nm) is considerably reduced (to 10–50 nm) as the consequence of the shrinkage of the "primary" gel particles caused by their dehydration.

The section-analysis of individual near-spheroidal-shaped particles (Figure 6) clearly indicates that the "primary" particles are not spheres, but discs having a mean diameter of about 80 nm and mean height of about 15 nm. In addition, knowing that the characteristic height of the growing terraces of low-silica zeolites (zeolite A, faujasite) is about 1.2–1.4 nm which corresponds to the sizes of the unit cells of the mentioned zeolites [4-7,40], appearing of the

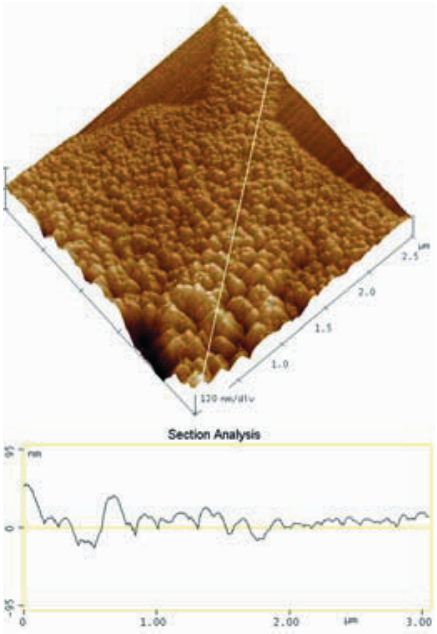

Figure 5. AFM image of the X-ray amorphous aluminosilicate precursor for the synthesis of zeolite A($t_c = 0$). Surface plot of height data taken in contact mode, scan size 2.5×2.5 μm, with corresponding topographic profile along indicated line ("section analysis").

vertical heights of 1.225 nm on some of the primary gel particles indicates the short-range ordering in the predominantly amorphous material. It seems that due to the high local supersaturation of constituents (Na, Si, Al) [12,13,41,42], the statistical conditions for the formation of not only amorphous phase, but also for

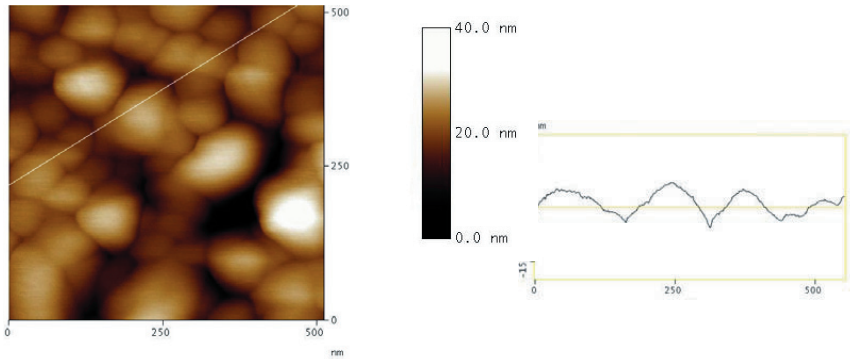

Figure 6. Typical AFM image of the elemental (unit) particles of the solid phase separated from a freshly prepared hydrogel used as precursor for the synthesis of zeolite A (gel; $t_c = 0$), on mica.

the gradual formation of short-medium-to-long-range ordering (Figure 5), can be realized in the certain regions of gel, during its formation.

4 Conclusion

Analyses of structural (by XRD, FTIR) and particulate properties (by SEM, TEM, and AFM) of the solid phase (gel) separated from freshly prepared hydrogel, $t_c = 0$, show for the gel precursor for the synthesis of silicalite-1 that: 1). Analysis of XRD pattern and FTIR spectrum of the gel indicated the presence of ordered pentasile structure, most probably 36T units of MFI structure, in the gel matrix 2) The size of smallest gel particles ($\leqslant 10$ nm) is the critical size at which a part of gel nutrient transforms into crystalline phase that can be both amorphous and crystalline. It is concluded that the $\leqslant 10$ nm particles are formed by fast reactions in the sequence: (i) formation of inorganic-organic composite species by reaction of silicate anions and TPA^+ ions, (ii) formation of primary $\sim$3 nm particles by aggregation of several inorganic-organic composite species and (iii) formation of $\leqslant 10$ nm particles by aggregation of several primary ($\sim$3 nm) particles, during the preparation of hydrogel. Further stepwise aggregation of such formed $\leqslant 10$ nm particles results in the formation of "hierarchically structured" gel precursor.

Analyses of the solid phase (gel) separated from freshly prepared hydrogel, $t_c = 0$, show for the gel precursor for the synthesis of zeolite A that the predominantly true amorphous phase of the gel contains small proportions of partially crystalline ("quasi-crystalline") or even fully crystalline phase. This finding is also confirmed by AFM. Namely three different entities can be observed in the AFM images of the freshly prepared gel; aggregate of disc-shaped particles (having the mean diameter of about 80 nm and mean height of about 15 nm.), "transition", probably partially crystalline, features (particles of "quasi-crystalline" phase) and aggregates of "pyramidal-shape" features which look like fully crystalline material. Since enlargement of the disc-shaped particles does not result in an observing of some "structural" particularities, it is concluded that just these particles represent the primary amorphous gel particles. Also is concluded that the "pyramidal-shaped" particles are zeolite nuclei.

Acknowledgements

This work is realized in the frame of the projects: A679007 and 0982934-2744 financially supported by the Ministry of Science, Education and Sport of the Republic of Croatia and the project CRO-03/2006 financially supported by the Hungarian Science and Technology Foundation. The authors gratefully acknowledge these financial supports.

References

[1] C.S. Cundy, P.A. Cox, *Microporous Mesoporous Mater.* **82** (2005) 1-78.

[2] R.M. Barrer, *Hydrothermal Chemistry of Zeolites, Academic Press*, London, 1982.

[3] B. Subotić, J. Bronić, In: *Handbook of Zeolite Science and Technology*, S.M. Auerbach, K.A. Carrado and P.K. Dutta (Eds.), Marcel Dekker Inc., New York–Basel (2003) pp. 129-203.

[4] M.W. Anderson, J.R. Agger, J.T. Thornton, N. Forsyth, *Angew. Chem. Int. Ed*. **35** (1996) 1210-1213.

[5] J.R. Agger, N. Pervaiz, A.K. Cheetham, M.W. Anderson, *J. Am. Chem. Soc*. **120** (1998) 10754-10759.

[6] S. Dumrul, S. Bazzana, J. Warzywoda, R.R. Biederman, A. Sacco Jr., *Microporous Mesoporous Mater.* **54** (2002) 79-88.

[7] T. Wakihara, T. Okubo, *J. Chem. Eng. Jpn*. **37** (2004) 669-674.

[8] R.W. Thompson, A. Dyer, *Zeolites* **5** (1985) 202-210.

[9] J.B. Nagy, P. Bodart, H. Collette, C. Fernandez, Z. Gabelica, A. Nastro, R. Aiello, *J. Chem. Soc. Faraday Trans*. **85** (1989) 2749-2769.

[10] J. Warzywoda, R.D. Edelman, R.W. Thompson, *Zeolites* **11** (1991) 318-324.

[11] G. Golemme, A. Nastro, J.B. Nagy, B. Subotić, F. Crea, R. Aiello, *Zeolites* **11** (1991) 776-783.

[12] L. Gora, K. Streletzky, R.W. Thompson, G.D.J. Phillies, *Zeolites* **19** (1997) 98-106.

[13] S. Mintova, N.H. Olson, V. Valtchev, T. Bein, *Science* **283** (1999) 958-960.

[14] L.A. Bursill, J.M. Thomas, In: *Recent Progress Report and Discussions: 5^{th} International Zeolite Conference*, R. Sersale, C. Collela, R. Aiello (Eds.), Giannini, Naples (1981) pp. 25.

[15] O. Okamura, Y. Tsuruta, T. Satoh, *Gypsum and Lime* **206** (1987) 23-28.

[16] R. Aiello, F. Crea, A. Nastro, B. Subotić, F. Testa, *Zeolites* **11** (1991) 767-775.

[17] B. Subotić, A. M. Tonejc, D. Bagović, A. Čižmek, T. Antonić, *Stud. Surf. Sci. Catal*. **84A** (1994) 259-266.

[18] E.M. Flanigen, D.W. Breck, Abstract of papers, In: *137th National Meeting of the ACS*, Cleavand OH, April 1960 (American Chemical Society, Washington, DC, 1960) INOR 82.

[19] S.P. Zhdanov, N.N. Samulevich, In: *Proceedings of the Fifth International Conference on Zeolites*, Naples, Italy, June 02-06, 1980; L.V.C. Rees (Ed.), Heyden, London-Philadelphia-Rheine (1980) pp. 75-84.

[20] C.E.A. Kirschkock, R. Ravishankar, P.A. Jacobs, J.A. Martens, J. Phys. Chem. B **103** (1999) 11021-11027.

[21] P.P.E.A. de Moor, T.P.M. Beelen, R.A. Van Santen, L.W. Beck. M.E. Davis, *J. Phys. Chem. B* **104** (2000) 7600-7611.

[22] D.P. Serrano, R. Van Grieken, *J. Mater. Chem*. **11** (2001) 2391-2407.

[23] H. Ramanan, E. Kokkoli, M. Tsapatsis, *Angew. Chem. Int. Ed.* **43** (2004) 4558-4561.

[24] A. Iwasaki, T. Sano, Y. Kiyozumi, *Microporous Mesoporous Mater.* **25** (1998) 119-126.

[25] E.M. Flanigen, *Proc. 5th International Zeolite Conference,* L.C.V. Rees (Ed.) Heyden, London (1980) 760.

[26] E.G. Derouane, S. Detremerrie, Z. Gabelica and N. Blom, *Appl. Catal.* **1** (1981) 201-224.

[27] P.-P.E.A. de Moor, T.P.M. Beleen, B.U. Komanschek, L.W. Beck, P. Wagner, M.E. Davis, R.A. van Santen, *Chem. Eur*. **5** (1999) 2083-2088.

[28] B.J. Schoeman, *Zeolites* **18** (1998) 97-105.

[29] P.A. Jacobs, E.D. Derouane, J. Weitkamp, *J. Chem. Soc., Chem. Commun*. (1981) 591-593.

[30] S. Mintova, N.H. Olson, J. Senker, T. Bein, *Angew. Chem. Int. Ed. Engl*. **41** (2002) 2558-2561.

[31] J.N. Watson, A.S. Brown, L.E. Iton, J.W. White, *J. Chem. Soc. Faraday Trans*. **94** (1998) 2181-2186.

[32] D. Lesthaeghe, P. Vansteenkiste, T. Verstraelen, A. Ghysels, C.E.A. Kirschhock, J.A. Martens, V. Van Speybroeck, M. Waroquier, *J. Phys. Chem.* **C112** (2008) 9186-9191.

[33] Y. Tsuruta, T. Satoh, T. Yoshida, O. Okumura, S. Ueda, S. In: *New Development in Zeolite Science, Studies in Surface Science and Catalysis* Vol. 28, Y. Murakami, A. Iijima, J.W. Ward (Eds.), Elsevier, Amasterdam, (1986) 1001.

[34] D.S. Kudasheva, J. Lai, A. Ulman, M.K. Cowman, *J. Inorg. Biochem.* **98** (2004) 1757–1769.

[35] V. Nikolakis, D.G Vlachos, M. Tsapatsis, *Microporous Mesoporous Mater*. **21** (1998) 337-346.

[36] P.-P.E.A. de Moor, The Mechanism of Organic-Mediated Zeolite Crystallization, Ph.D. Thesis, Tecnical University of Eindhoven, Eindhoven, The Netherlands (1998).

[37] W.H. Dokter, H.F. van Garderen, T.P.M Beleen, R.A. van Santen, V. Bras, *Angew. Chem. Int. Ed. Engl*. **34** (1995) 73-75.

[38] O. Regev, Y. Cohen, E. Kehat, Y. Talmon, em Zeolites **14** (1994) 314-319.

[39] B. Subotić, J. Bronić, T. Antonić Jelić, In: *Ordered Porous Solids*, V. Valtchev, S. Mintova, M. Tsapatsis (Eds), Elsevier, Amsterdam (2008) p. 127.

[40] J.R. Agger, M.W. Anderson, *Stud. Surf. Sci. Catal*. **142A** (2002) 93-100.

[41] Y. Yan, S.R. Chaudhuri, A. Sarkar, *Chem. Mater*. **8** (1996) 473-497.

[42] L. Gora, K. Streletzky, R.W. Thompson, G.D.J. Phillies, *Zeolites* **18** (1997) 119-131.